Frontiers of Physics
https://doi.org/10.1007/s11467-021-1054-0
Front. Phys.
16(4), 43203 (2021)

Topical Review

Theoretical progress on direct Z-scheme photocatalysis of two-dimensional heterostructures

Zhaobo Zhou, Shijun Yuan†, Jinlan Wang‡

School of Physics, Southeast University, Nanjing 211189, China
Corresponding authors. E-mail: †siesta@seu.edu.cn, ‡jlwang@seu.edu.cn
Received October 17, 2020; accepted January 2, 2021

Two-dimensional (2D) materials, due to its excellent mechanical, unique electrical and optical properties, have become hot materials in the field of photocatalysis. Especially, 2D heterostructures can well inhibit the recombination of photogenerated electrons and holes in photocatalysis because of its special energy band structures and carrier transport characteristics, which are conducive to enhancing photoenergy conversion capacity and improving oxidation and reduction ability, so as to purify pollutants and store energy. In this minireview, we summarize recent theoretical progress in direct Z-scheme photocatalysis of 2D heterostructures, focusing on physical mechanism and improving catalytic efficiency. Current challenges and prospects for 2D direct Z-scheme photocatalysts are discussed as well.

Keywords two-dimensional heterostructures, direct Z-scheme, photocatalyst, density functional theory

Contents

1 Introduction 1
2 Heterojunction structural models and computational methods 2
3 Rational design of 2D direct Z-scheme photocatalysts 3
3.1 Band alignment 3
3.2 Internal electric field 4
3.3 Band position 4
3.4 Charge transfer dynamics 5
4 Summary and outlook 6
Acknowledgements 7
References 7

1 Introduction

The use of energy transmitted by photons to initiate and/or drive chemical reactions is called photocatalysis [1, 2]. The most common in nature is photosynthesis, which is driven by visible light. Solar-driven photocatalysis is considered to be an effective way to solve the problem of energy shortage and environmental pollution [3, 4]. In view of this, various trial-and-error experimental attempts have been carried out in preparation of high-efficiency photocatalysts, but the narrow visible light response range and low quantum efficiency of photocatalysts still restrict their development and practical application [5–10]. During the past decades, various theoretical studies have been focused on artificial design of high efficiency photocatalysts, which accelerate the development of this field [11–22]. Generally, a valuable photocatalyst should meet at least three fundamental requirements at the same time, that is, high light absorption efficiency in the visible range, strong photocatalytic activity, and robust photoresist stability [23]. However, all of them are often in conflict with each other and hard to be reconciled. For example, in order to improve the catalytic performance, the catalytic sites should be active enough, which often makes the active sites unable to withstand the structural deformation caused by light corrosion or thermal disturbance. Moreover, some nanoparticle catalysts expose very high initial catalytic performance, while the catalytic activity attenuates rapidly due to their poor stability [24]. To overcome this problem, two-dimensional (2D) semiconductor materials have been widely utilized in the field of photocatalysis due to their inherent advantages such as their ultra-thin layered structure, large specific surface area, high density of surface active sites, and excellent mechanical properties [25–27]. Moreover, unlike bulk materials, photogenerated carriers in 2D semiconductor materials can be directly generated on the surface, leading to faster interfacial transmission and shorter diffusion path. Therefore, 2D semiconductor nanomaterials have broad application prospects as photocatalysts.

Beyond single 2D semiconductors, heterogeneous junctions formed by stacking various 2D materials not only

*Special Topic: Heterojunction and Its Applications (Ed. Chenghua Sun). This article can also be found at http://journal.hep.com.cn/fop/EN/10.1007/s11467-021-1054-0.

allow a broader range of solar light absorption but also promote the special separation of photogenerated carriers, thus attracting tremendous interest for photocatalytic applications. Two main ways including horizontal or vertical stacking have been exploited to construct 2D heterojunctions, which can be classified as in-plane heterojunctions and out-of-plane heterojunctions. In particular, the vertical out-of-plane stacked heterojunctions are like LEGO bricks, which can be assembled into various structures with different functionalities. Note that vertical heterojunctions can not only retain the outstanding properties of single components due to the weak van der Waals (vdW) interlayer coupling, but also bring about some novel physics characteristics that do not exist in a single 2D material. For instance, the h-BN acting as a substrate can improve the mobility and carrier inhomogenety of graphene by more than ten times in h-BN/graphene heterostructures [28]. MoS_2/WSe_2 and MoS_2/WS_2 heterojunctions can produce exciting interlayer excitons [29]. To date, thousands of 2D materials have been predicted through computational screening, which provides a wealth of choices for the rational design of 2D heterojunctions [30].

Currently, engineering 2D heterojunctions to design artificial photocatalysts has become a new research field. By stacking different types of 2D materials, they can be classified as semiconductor–metal (S–M) heterostructure photocatalysts and semiconductor-semiconductor (S–S) heterostructure photocatalysts. For 2D S–M heterostructure photocatalysts, the photogenerated electrons can transfer rapidly from semiconductor to metal due to the metal conductivity [31, 32], avoiding the recombination of photogenerated electrons and holes in semiconductor materials. For 2D S–S heterostructure photocatalysts, besides the efficient separation of photoexcited electrons and holes, photoccarriers can be generated in both two semiconductors to participate in catalytic reaction, thus improving the quantum yield of photocatalyst. According to the charge carrier transfer modes, 2D S–S heterostructure photocatalysts can be divided as type-II and Z-scheme [23]. In particular, effective charge separation and redox ability can be realized simultaneously in Z-scheme system. As a valid strategy to improve photocatalysis, Z-scheme photocatalysts can be further divided into three types depending on whether the carrier transfer mediator is introduced or not: traditional Z-scheme photocatalysts, all-solid-state Zscheme photocatalysts and direct Z-scheme photocatalysts. Among them, direct Z-scheme photocatalysts can effectively avoid the backward reactions and the light-shielding effect caused by the carrier transfer mediators [33, 34], thus becoming the hotspot of current photocatalytic application. In this minireview, we focus on theoretical design of 2D direct Z-scheme photocatalysts, believing that it can stimulate more in-depth theoretical research and provide possible opportunities for experimental work on photocatalysis.

2 Heterojunction structural models and computational methods

From a calculation viewpoint, a reliable structure model of vertical heterojunctions needs to be constructed before performing calculations. This is usually a challenge because 2D materials normally have different lattice constants. To achieve a low lattice mismatch, one approach is to rotate one layer and make the lattice constants close as much as possible [35]. However, this approach requires constructing a supercell and the size of supercell may be very large for a reasonable lattice match. Fortunately, with the development of computer performance, the computational cost of electronic structure calculations for a supercell containing 100 atoms or more is now affordable. Another approach is to apply a small amount of in-plane strain on the 2D material, as implemented in SnS_2/g-C_3N_4 heterojunctions [36]. The in-plane strain of 1% was applied to keep SnS_2 monolayer matching well with g-C_3N_4 monolayer. In general, these two methods are usually adopted together in constructing model of 2D heterojunctions, which favors to keep the lattice mismatch in a reasonable range (<3%) without a large supercell. As a consequence, we can obtain accurate theoretical results with an acceptable computational cost..

Band structures and work function of materials are the most important properties for designing 2D heterojunctions photocatalysts. First-principles calculation based on density functional theory (DFT) is a powerful theoretical tool for predicting the structural, electronic and optical properties of 2D semiconductor materials. In particular, DFT calculations with the HSE06 hybrid functional [37, 38] have been demonstrated to reproduce accurate band structures and lattice parameter correction of 2D vdW heterojunctions.

Therefore, by means of DFT method, we can theoretically design 2D direct Z-scheme photocatalysts by calculating work function and charge density difference. The work function W is defined as the energy barrier that the electron at the Fermi level escapes from the solid to the surface. It can be expressed as follows [39]:

$$W = E_{\mathrm{vac}} - E_{\mathrm{F}}. \tag{1}$$

Here E_{vac} and E_{F} represent the vacuum level and Fermi level respectively. The E_{vac} can be acquired by calculating the electrostatic potential. The charge density difference can be calculated as follows:

$$\Delta\rho = \rho_{A/B} - \rho_A - \rho_B. \tag{2}$$

Here $\rho_{A/B}$, ρ_A and ρ_B represent the charge density of A/B vdW heterostructure, A monolayer and B monolayer, respectively. The calculated work function and charge density difference determine the internal electric field direction at the surface of heterostructure, which is essential

for judging whether the photogenerated charge transfer along Z-scheme mode.

In 2D heterojunctions, an accurate description of the distance between the two layers is also important. This involves not only whether photogenerated electrons or holes can transition between layers, but also slightly affects the electron states of the 2D heterojunctions near the Fermi level. Although the exchange-correlation functional of generalized gradient approximation [40] has been widely used in the prediction of solid lattice constants, its description of long-range weak interaction is deficient. Fortunately, there are many ways to solve this problem, such as the semi-empirical PBE+D (D stands for dispersion) correction proposed by Grimme [41] and the non-empirical van der Waals density functional (vdW-DF) scheme proposed by Dion *et al.* [42]. The development of these theoretical tools provides powerful technical support for the exploration of the photocatalytic properties of 2D heterojunction materials.

3 Rational design of 2D direct Z-scheme photocatalysts

In general, the direct Z-scheme photocatalyst is composed by stacking one oxidation reaction semiconductor photocatalyst (ORP) with one reduction reaction semiconductor photocatalyst (RRP), both of them can induce photogenerated electron–hole (e–h) pairs under sunlight. The excited electrons in the conduction band (CB) of RRP and the holes in the valence band (VB) of ORP are preserved, while the excited electrons in the CB of ORP will recombine with the holes in the VB of RRP, forming a series of electron transfer chains that make a "Z" [43]. Hence, the photogenerated electrons and holes with the strongest reduction and oxidation abilities can be created and participated in specific reactions such as pollutant degradation, water splitting, and CO_2 reduction [44, 45]. From this perspective, in terms of the rational design of high-efficiency 2D direct Z-scheme photocatalysts in theory, two critical issues need to be taken into consideration: efficient separation of photoexcited e–h pairs and strong redox ability, which are strongly decided by band alignment, internal electric field, band position as well as charge transfer dynamics.

3.1 Band alignment

The constructed semiconductor heterostructures should exhibit staggered band alignment to meet the requirement that induces the spatial separation of photoexcited e–h pairs. As shown in Fig. 1, there are three types of typical band alignment named type-I, type-II and type-III. For the type-I band alignment, the CB and VB levels of semiconductor A are higher and lower than corresponding bands of semiconductor B, respectively. As a result, the photogenerated electrons will accumulate at the CB levels and the photogenerated holes will accumulate at VB levels of semiconductor B, and the redox reaction will occur at semiconductor B. For the type-II band alignment, the CB and VB levels are all higher than corresponding levels of semiconductor B. Thus, an efficient photogenerated e–h separation is achieved and the redox reaction would take place on the corresponding semiconductors [46]. The type-III band alignment is different from the type-I and type-II ones owing to no bandgap overlap. Therefore, the e–h separation between the two semiconductors cannot occur for the type-III band alignment [47]. Among aforementioned analysis, it is clear that only type-II band alignment is suitable for designing 2D direct Z-scheme photocatalysts because of its efficient separation of photogenerated e–h pairs. Note that type-II band alignment is suitable not only for direct Z-scheme photocatalysts, but also for traditional heterojunction photocatalysts [48, 49]. As shown in Fig. 1(b), the photogenerated electrons in CB of semiconductor A will transfer to the corresponding level of semiconductor B and the photogenerated holes follow a reverse migration, resulting in a traditional type-II charge transfer path instead of Z-scheme. This means band alignment is only the prerequisite for the Z-scheme system, and other factors must be considered to evaluate the charge transfer mode.

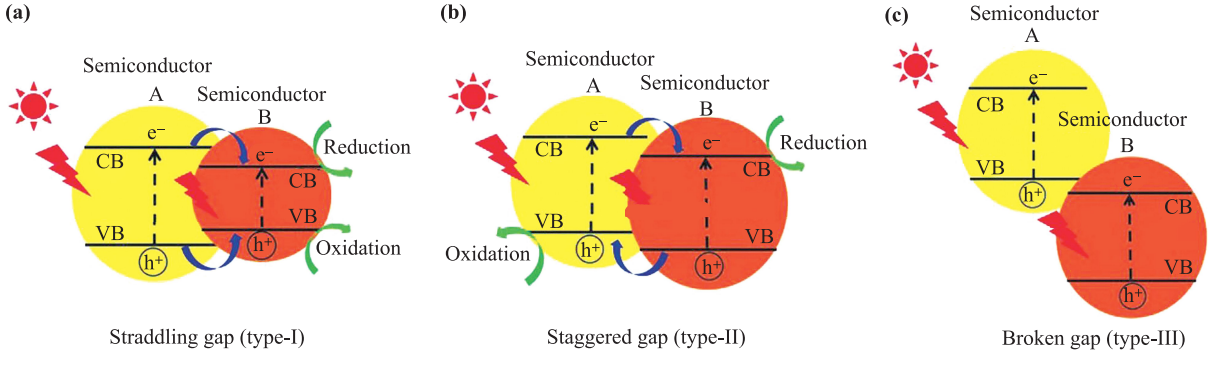

Fig. 1 Schematic illustration of three different band alignment of e–h pairs in the case of conventional light-responsive heterojunction photocatalysts: **(a)** type-I, **(b)** type-II, and **(c)** type-III. Reproduced with permission from Ref. [18].

3.2 Internal electric field

Internal electric field provides the driving force that affects the photogenerated carriers transfer path between two semiconductors, which plays an important role in the design of 2D direct Z-scheme photocatalyst. Two different processes can be expressed as follows: after two semiconductors are put into contact, the free electrons of photocatalyst (PC) I with a smaller work function (W_1) will transfer to PC II with a larger work function (W_2) until the Fermi level is equilibrated [Fig. 2(a)]. As a result, negative charges accumulate in PC II while positive charges accumulate in PC I at the interface, and an internal electric field is formed pointing from PC I to PC II [Fig. 2(b)]. Under the light irradiation, the photogenerated electrons in CB of PC II will recombine with holes in VB of PC I by means of the driving force of internal electric field [Fig. 2(c)]. Moreover, the photogenerated electrons transfer from CB of PC I to CB of PC II and photogenerated holes transfer from VB of PC II to VB of PC I, as well as photogenerated e–h recombination between the CB of PC I and VB of PC II, will be impeded [Figs. 2(d) and (e)]. In this case, the Z-scheme charge transfer path is preferred, and the reduction and oxidation reactions will occur at CB of PC I and VB of PC II with stronger catalytic ability, respectively. Different from the first case, if a 2D n-type semiconductor with a smaller work function (W_2) is in contact with a 2D p-type semiconductor with a larger work function (W_1), constructing p–n junction [Fig. 3(a)], the free electrons will flow from Fermi level of n-type semiconductor to Fermi level of p-type semiconductor. Under this circumstance, positive and negative charge will accumulate at the n-type side and p-type side respectively, forming an internal electric field pointing from n-type semiconductor to p-type semiconductor [Fig. 3(b)]. When exposing to the light irradiation, the photogenerated electrons will spontaneously transfer from higher CB to lower CB, and holes transfer from lower VB to higher VB in the p–n junction [Fig. 3(c)]. Meanwhile, the photogenerated e–h recombination between CB of n-type semiconductor and VB of p-type semiconductor will be inhibited due to the repulsive effect of the internal electric field [Fig. 3(d)]. Such an unfavorable charge transfer mode indicates that traditional p–n junction is not suitable for the design of 2D direct Z-scheme photocatalyst.

3.3 Band position

Generally, direct Z-scheme photocatalysts exhibit stronger redox ability than that of traditional heterojunction photocatalysts. This can be attributed to that the photogenerated electrons and holes will reside in the higher CB and the lower VB respectively to participate in the subsequent reduction and oxidation reaction. However, from thermodynamic viewpoint, an appropriate band position is the prerequisite for the catalytic reaction to take place. For example, to achieve overall water splitting on a 2D semiconductor, its CB potential must be more negative than that of H_2 generation (−0.42 V vs. NHE at pH 7) and its VB potential must be more positive than that required for O_2 generation (0.81 V vs. NHE at pH 7) [51–53], as shown in Fig. 4(a). Otherwise, the corresponding catalytic reaction will not occur. For overall water splitting on direct Z-scheme heterostructure, however, it is not necessary to meet the above requirements. In Fig. 4(b), Ren *et al.* reported PtS_2/arsenene vdW heterostructure as an efficient direct Z-scheme photocatalyst for overall water splitting [54]. The CB potential of PtS_2 locates below the H_2 generation potential and the VB potential of arsenene locates above the O_2 generation potential, revealing that only H_2 evolution and O_2 evolution half-reaction instead of overall water splitting occurs on two semiconductor layers respectively. Thus, a reasonable direct Z-scheme photocatalyst must ensure that the lower VB locates below the oxidation potential and the higher CB locates above the reduction potential. Furthermore, the energy differ-

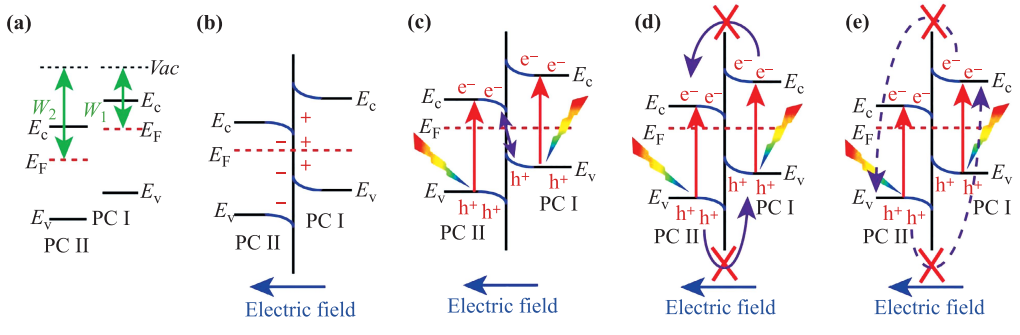

Fig. 2 Schematic illustration of semiconductor-semiconductor junction with staggered band configurations: **(a)** before contact, **(b)** in contact, **(c)** photogenerated carrier transfer process in direct Z-scheme mode, **(d)** photogenerated carrier transfer process in type-II mode, and (e) photogenerated carrier recombination. W_1 and W_2 denote the work function of PC I and PC II, respectively. V_{ac}, E_c, E_v, and E_F stand for the vacuum level, conduction band minimum, valence band maximum, and Fermi level, respectively. Reproduced with permission from Ref. [50].

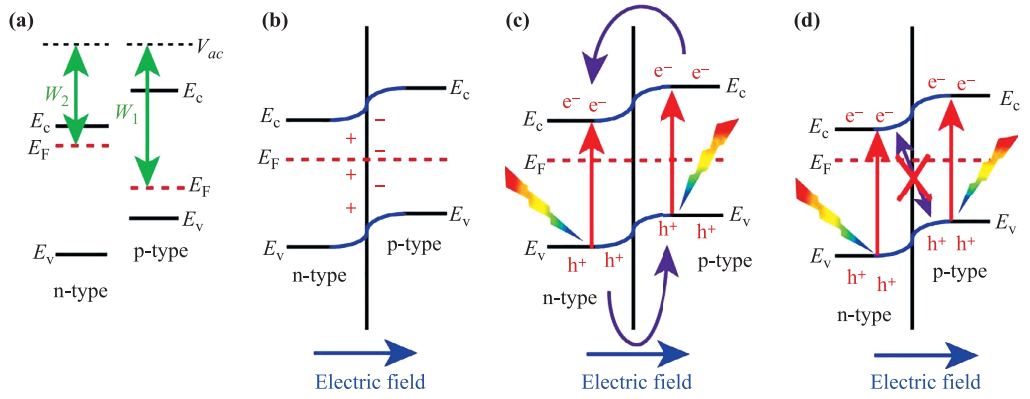

Fig. 3 Schematic illustration of p–n junction: **(a)** before contact, **(b)** in contact, **(c)** transfer of photogenerated carriers in p–n junction mode, and **(d)** not allowed transfer of photogenerated carriers in direct Z-scheme mode. Reproduced with permission from Ref. [50].

ence between CB (VB) potential and reduction (oxidation) potential, ΔE_{over}, is also a key factor limiting the photocatalytic efficiency of the redox reaction. Comparable to activation barriers that need to be overcomed in classical (thermal) heterogeneous catalysis by providing thermal energy, a sufficient ΔE_{over} needs to be provided in photocatalytic reactions to achieve high reaction rates. For example, for O_2 evolution reaction, the overpotential η should meet the following formula [55]:

$$\eta = \Delta G_{max} - 1.23\ \text{eV}, \tag{3}$$

here the ΔG_{max} represents the Gibbs free energy difference of rate-limiting step, and 1.23 eV is the equilibrium potential. Only when the ΔE_{over} is above the η, the photocatalyst can facilitate the water oxidation. Thus, a good 2D direct Z-scheme photocatalyst not only requires the more negative CB potential (positive VB potential) of 2D semiconductor as compared with reduction (oxidation) reaction potential, but a considerable ΔE_{over} is also needed to overcome the energy barrier derived from Gibbs free energy difference of rate-limiting step.

3.4 Charge transfer dynamics

When electron is excited under sunlight, the photogenerated e–h recombination and charge transfer also occur during the catalytic reactions. Therefore, more attention should be paid to the dynamic process of photogenerated electrons or holes. Recently, some groups have utilized nonadiabatic molecular dynamics simulations to explore the photogenerated charge transfer dynamics processes of 2D heterostructures for the design of 2D direct Z-scheme photocatalysts [33, 56, 57]. The strategy is as follows: the photogenerated charge transfer in heterostructure with type-II band alignment involves three significant processes: ① photogenerated carriers separation between heterostructure, ② interlayer e–h recombination and ③ intralayer e–h recombination, as shown in Fig. 5(a). Note that the effect of band bending on photogenerated electron and hole is not taken into consideration because the concept of band bending near an interface does not apply for atomically thin layers [58]. These processes occur in parallel and compete with each other. Thus, the competitive relationship between these dynamics processes signifi-

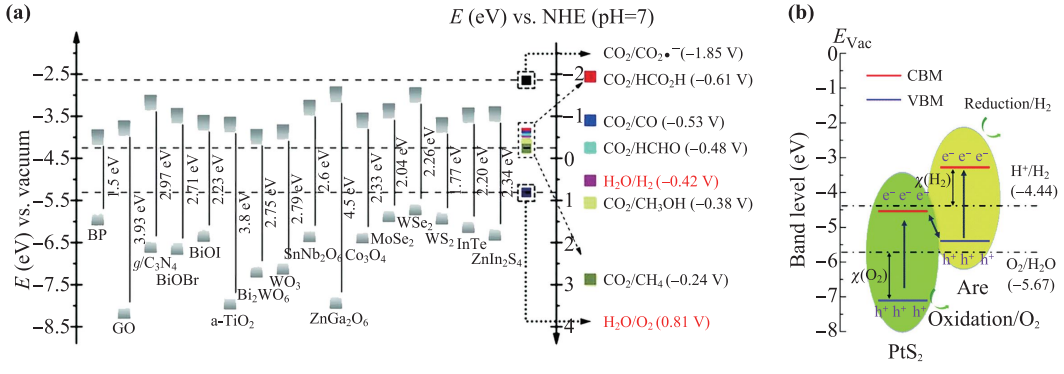

Fig. 4 **(a)** Band positions and potential applications of some common 2D materials versus NHE at pH 7. Reproduced with permission from Ref. [53]. **(b)** Band position of PtS_2/arsenene vdW heterostructure and the potentials of oxidation (O_2/H_2O) and reduction (H^+/H_2) at pH=0. Reproduced with permission from Ref. [54].

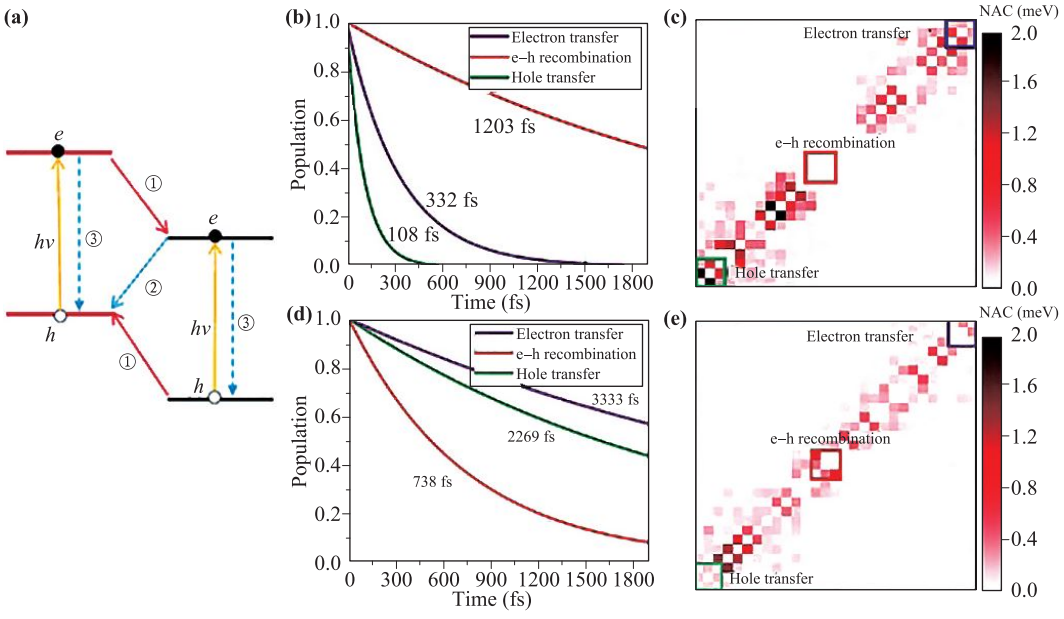

Fig. 5 **(a)** Schematic diagram of photoexcitation and charge transfer dynamics at $MoSe_2/MoS_2$ interface: ① electron and hole transfer between heterostructure, ② interlayer e–h recombination and ③ intralayer e–h recombination. Reproduced with permission from Ref. [59]. **(b, d)** Electron transfer, hole transfer and e–h recombination dynamics of MoSSe/WSeTe heterostructures with Te–Se and Te–S stacking. The time data are fitted by $f(t) = \exp((-t)/\tau)$ **(c)** and **(e)** averaged values of NAC between different states for Te–Se and Te–S stacking. The color bar suggests the coupling strength: the deeper the color is, the stronger the coupling is. Reproduced with permission from Ref. [33].

cantly affects the photogenerated charge transfer path via traditional type-II mode or Z-scheme mode. In particular, Zhao *et al.* reported 2D BCN/C_2N heterostructure as a direct Z-scheme photocatalyst for water splitting due to its ultrafast interlayer e–h recombination (process ②) as compared with intralayer e–h recombination (process ③) [56]. Our group demonstrated that 2D MoSSe/WSeTe vdW heterostructures is a promising direct Z-scheme photocatalyst for hydrogen evolution by comparing the relationship between charge transfer rate and interlayer e–h recombination lifetime [Figs. 5(b)–(e)] [33]. It can be seen that the electron transfer (332 fs) and hole transfer (108 fs) are much faster than that of e–h recombination (1203 fs) for Te–Se stacking [Fig. 5(b)], revealing its type-II mode. In contrast, for Te–S stacking, the e–h recombination (738 fs) exhibits a faster time scale as compared with the electron transfer (3333 fs) and hole transfer (2269 fs), which makes charge transfer facilitate the Z-scheme mode [Fig. 5(d)]. These results are also demonstrated by the averaged nonadiabatic coupling (NAC). The larger the NAC is, the faster the charge transfer or e–h recombination is. These studies revealed that if the lifetime of process ② is much shorter than that of processes ① and ③, the photogenerated electrons and holes would flow along Z-scheme charge transfer path. Otherwise, it behaves as traditional type-II path. Such charge transfer dynamics processes, however, cannot be described well by regular DFT methods yet. This implies that to provide a more reliable criterion for the design of 2D direct Z-scheme photocatalysts, excited state methods such as nonadiabatic molecular dynamics should be further considered.

4 Summary and outlook

In summary, this review presents the strategies of improving heterostructure models and optimizing traditional computational methods, as well as crucial design criteria involving both ground state and excite state properties for theoretical exploration of 2D direct Z-scheme photocatalysis. The influence factors including band alignment, internal electric field, band position, and charge transfer dynamics are the key features for the design of potential 2D direct Z-scheme photocatalysts. First, the constructed semiconductor heterostructures need to exhibit type-II band alignment. Second, the direction of internal electric field should be consistent with photogenerated e–h recombination from lower CB to higher VB at the interface. Third, the interlayer e–h recombination should be much faster than intralayer e–h recombination and photogenerated carriers separation. Only when the heterostructure system meets above requirements, the Z-scheme charge transfer mode can be established. Otherwise, it tends to be traditional type-II charge transfer mode. Also, to ensure that the strong redox reaction can occur, the CB potential of the reduction layer and the VB potential of the oxidation layer in 2D direct Z-scheme photocatalyst should be more negative and positive than the reduction

and oxidation reaction potential respectively. Meanwhile, the considerable energy difference between CB (VB) potential and reduction (oxidation) potential is needed to overcome the Gibbs free energy difference of the rate-limiting step. Based on the aforementioned conditions, the 2D direct Z-scheme photocatalyst can be effectively and reliably designed.

Besides the above discussions in this review, some challenges exist in the theoretical exploration of 2D direct Z-scheme photocatalyst. First, most theoretical studies of 2D direct Z-scheme photocatalysts are still focused on the calculations of band position, internal electric field and band alignment. But a good photocatalyst should own not only the physical criteria but also chemical properties (such as low overpotential) for it to be realized in experiments. Thus, the systematic calculations for catalytic activity of selected oxidation and reduction layers in 2D direct Z-scheme photocatalyst should be carried out to provide a comprehensive and reliable conclusion for the experiment.

Second, the surface of oxidation and reduction layers in 2D direct Z-scheme photocatalyst must be rationally controlled. In general, surface defects (e.g., vacancy, doping and atom reconfiguration) can serve as the catalytic active sites of 2D photocatalyst, thus improving the photocatalytic performance. However, they also significantly affect the photogenerated charge dynamics processes of the interface due to their atomic-level thickness, and the induced trap states in the bandgap would become as recombination-active center and speed up the e–h recombination. Therefore, the synergistic relationship between positive and negative factors of the surface properties seems to determine the practical application of 2D direct Z-scheme photocatalysis and tremendous research activities are still desired.

Third, the mechanisms of 2D direct Z-scheme photocatalysts remain largely unclear based on DFT and some novel theoretical simulation methods should be further developed. Recently, the nonadiabatic molecular dynamics simulation based on time-domain density functional theory has been exploited in design of 2D direct Z-scheme photocatalysts. By means of this method, we can explore the photoexcited carriers dynamics processes, which cannot be achieved by the traditional DFT method. Nevertheless, this method still shows some shortages including the lack of exciton effect and spin–orbit coupling, as well as the nuclear quantum effects, which may affect the calculated dynamics results. Therefore, extensive efforts are still needed on the further development of method to design 2D direct Z-scheme photocatalysts more accurately. We believe that the exploration of these problems can shed light on the effective and accurate design of novel 2D direct Z-scheme photocatalysts.

Acknowledgements This work was supported by the National Key R&D Program of China (No. 2017YFA0204800), the National Natural Science Foundation of China (Nos. 22033002, 21525311, and 21973011), and the Scientific Research Foundation of Graduate School of Southeast University (No. YBPY1968).

References

1. J. Di, J. Xiong, H. Li, and Z. Liu, Ultrathin 2D photocatalysts: Electronic-structure tailoring, hybridization, and applications, *Adv. Mater.* 30(1), 1704548 (2018)
2. J. D. Xiao and H. L. Jiang, Metal–organic frameworks for photocatalysis and photothermal catalysis, *Acc. Chem. Res.* 52(2), 356 (2019)
3. T. Su, Z. Liu, Y. Liang, Z. Qin, J. Liu, and Y. Huang, Preparation of PbYO composite photocatalysts for degradation of methyl orange under visible-light irradiation, *Catal. Commun.* 18, 93 (2012)
4. Z. Zhao, H. An, J. Lin, M. Feng, V. Murugadoss, T. Ding, H. Liu, Q. Shao, X. Mai, N. Wang, H. Gu, S. Angaiah, and Z. Guo, Progress on the photocatalytic reduction removal of chromium contamination, *Chem. Rec.* 19(5), 873 (2019)
5. B. Luo, G. Liu, and L. Wang, Recent advances in 2D materials for photocatalysis, *Nanoscale* 8(13), 6904 (2016)
6. Y. Huang, H. Xu, H. Yang, Y. Lin, H. Liu, and Y. Tong, Efficient charges separation using advanced BiOI-based hollow spheres decorated with palladium and manganese dioxide nanoparticles, *ACS Sustain. Chem. & Eng.* 6(2), 2751 (2018)
7. T. Su, R. Peng, Z. D. Hood, M. Naguib, I. N. Ivanov, J. K. Keum, Z. Qin, Z. Guo, and Z. Wu, One-step synthesis of Nb_2O_5/C/Nb_2C (MXene) composites and their use as photocatalysts for hydrogen evolution, *ChemSusChem* 11(4), 688 (2018)
8. X. Ma, D. Jiang, P. Xiao, Y. Jin, S. Meng, and M. Chen, 2D/2D heterojunctions of WO_3 nanosheet/$K^+Ca_2Nb_3O_{10}^-$ ultrathin nanosheet with improved charge separation efficiency for significantly boosting photocatalysis, *Catal. Sci. Technol.* 7(16), 3481 (2017)
9. Y. R. Lv, R. K. He, Z. Y. Chen, X. Li, and Y. H. Xu, Fabrication of hierarchical copper sulfide/bismuth tungstate p–n heterojunction with two-dimensional (2D) interfacial coupling for enhanced visible-light photocatalytic degradation of glyphosate, *J. Colloid Interface Sci.* 560, 293 (2020)
10. Y. Bao and K. Chen, Novel Z-scheme BiOBr/reduced graphene oxide/protonated g-C_3N_4 photocatalyst: Synthesis, characterization, visible light photocatalytic activity and mechanism, *Appl. Surf. Sci.* 437, 51 (2018)
11. L. Ju, Y. Dai, W. Wei, M. Li, and B. Huang, DFT investigation on two-dimensional GeS/WS_2 van der Waals heterostructure for direct Z-scheme photocatalytic overall water splitting, *Appl. Surf. Sci.* 434, 365 (2018)
12. C. F. Fu, R. Zhang, Q. Luo, X. Li, and J. Yang, Construction of direct Z-Scheme photocatalysts for overall water splitting using two-dimensional van der waals heterojunctions of metal dichalcogenides, *J. Comput. Chem.* 40(9), 980 (2019)

13. B. Wang, X. Wang, H. Yuan, T. Zhou, J. Chang, and H. Chen, Direct Z-scheme photocatalytic overall water splitting on two dimensional $MoSe_2/SnS_2$ heterojunction, *Int. J. Hydrogen Energy* 45(4), 2785 (2020)
14. P. Xia, B. Zhu, B. Cheng, J. Yu, and J. Xu, 2D/2D g-C_3N_4/MnO_2 nanocomposite as a direct Z-scheme photocatalyst for enhanced photocatalytic activity, *ACS Sustain. Chem. & Eng.* 6(1), 965 (2018)
15. Y. Lee, Y. Hwang, and Y. C. Chung, Achieving type I, II, and III heterojunctions using functionalized MXene, *ACS Appl. Mater. Interfaces* 7(13), 7163 (2015)
16. Z. Li, J. Hou, B. Zhang, S. Cao, Y. Wu, Z. Gao, X. Nie, and L. Sun, Two-dimensional Janus heterostructures for superior Z-scheme photocatalytic water splitting, *Nano Energy* 59, 537 (2019)
17. B. Wang, H. Yuan, J. Chang, X. Chen, and H. Chen, Two dimensional $InSe/C_2N$ van der Waals heterojunction as enhanced visible-light-responsible photocatalyst for water splitting, *Appl. Surf. Sci.* 485, 375 (2019)
18. J. Low, J. Yu, M. Jaroniec, S. Wageh, and A. A. Al-Ghamdi, Heterojunction photocatalysts, *Adv. Mater.* 29(20), 1601694 (2017)
19. S. Shen, and S. S. Mao, Nanostructure designs for effective solar-to-hydrogen conversion, *Nanophotonics* 1(1), 31 (2012)
20. B. Chen, P. Li, S. Zhang, W. Zhang, X. Dong, F. Xi, and J. Liu, The enhanced photocatalytic performance of Z-scheme two-dimensional/two-dimensional heterojunctions from graphitic carbon nitride nanosheets and titania nanosheets, *J. Colloid Interface Sci.* 478, 263 (2016)
21. B. Xia, F. Deng, S. Zhang, L. Hua, X. Luo, and M. Ao, Design and synthesis of robust Z-scheme ZnS-SnS_2 n–n heterojunctions for highly efficient degradation of pharmaceutical pollutants: Performance, valence/conduction band offset photocatalytic mechanisms and toxicity evaluation, *J. Hazard. Mater.* 392, 122345 (2020)
22. Y. Liu, P. Lv, W. Zhou, and J. Hong, Built-in electric field hindering photogenerated carrier recombination in polar bilayer SnO/BiOX (X = Cl, Br, I) for water splitting, *J. Phys. Chem. C* 124(18), 9696 (2020)
23. T. Su, Z. Qin, H. Ji, and Z. Wu, An overview of photocatalysis facilitated by 2D heterojunctions, *Nanotechnology* 30(50), 502002 (2019)
24. X. Chen, R. Hu, and F. Sun, Particle size effect of Ag catalyst for oxygen reduction reaction: Activity and stability, *J. Renew. Sustain. Energy* 10(5), 054301 (2018)
25. J. Liu, Y. Liu, N. Liu, Y. Han, X. Zhang, H. Huang, Y. Lifshitz, S. T. Lee, J. Zhou, and Z. Kang, Metal-free efficient photocatalyst for stable visible water splitting via a two-electron pathway, *Science* 347(6225), 970 (2015)
26. X. Lv, W. Wei, Q. Sun, F. Li, B. Huang, and Y. Dai, Two-dimensional germanium monochalcogenides for photocatalytic water splitting with high carrier mobility, *Appl. Catal. B* 217, 275 (2017)
27. D. Er, H. Ye, N. C. Frey, H. Kumar, J. Lou, and V. B. Shenoy, Prediction of enhanced catalytic activity for hydrogen evolution reaction in janus transition metal dichalcogenides, *Nano Lett.* 18(6), 3943 (2018)
28. A. K. Geim and I. V. Grigorieva, Van der Waals heterostructures, *Nature* 499(7459), 419 (2013)
29. P. Rivera, H. Yu, K. L. Seyler, N. P. Wilson, W. Yao, and X. Xu, Interlayer valley excitons in heterobilayers of transition metal dichalcogenides, *Nat. Nanotechnol.* 13(11), 1004 (2018)
30. S. Haastrup, M. Strange, M. Pandey, T. Deilmann, P. S. Schmidt, N. F. Hinsche, M. N. Gjerding, D. Torelli, P. M. Larsen, and A. C. Riis-Jensen, The computational 2D materials database: High-throughput modeling and discovery of atomically thin crystals, *2D Mater.* 5, 042022 (2018)
31. K. Roy, M. Padmanabhan, S. Goswami, T. P. Sai, G. Ramalingam, S. Raghavan, and A. Ghosh, Graphene-MoS_2 hybrid structures for multifunctional photoresponsive memory devices, *Nat. Nanotechnol.* 8(11), 826 (2013)
32. M. Bernardi, M. Palummo, and J. C. Grossman, Extraordinary sunlight absorption and one nanometer thick photovoltaics using two-dimensional monolayer materials, *Nano Lett.* 13(8), 3664 (2013)
33. Z. Zhou, X. Niu, Y. Zhang, and J. Wang, Janus MoSSe/WSeTe heterostructures: a direct Z-scheme photocatalyst for hydrogen evolution, *J. Mater. Chem. A* 7(38), 21835 (2019)
34. K. Maeda, Z-scheme water splitting using two different semiconductor photocatalysts, *ACS Catal.* 3(7), 1486 (2013)
35. W. Hu and J. Yang, First-principles study of two-dimensional van der Waals heterojunctions, *Comput. Mater. Sci.* 112, 518 (2016)
36. J. Liu and E. Hua, High photocatalytic activity of heptazine-based g-C_3N_4/SnS_2 heterojunction and its origin: insights from hybrid DFT, *J. Phys. Chem. C* 121(46), 25827 (2017)
37. J. Heyd, G. E. Scuseria, and M. Ernzerhof, Hybrid functionals based on a screened Coulomb potential, *J. Chem. Phys.* 118(18), 8207 (2003)
38. J. Heyd, G. E. Scuseria, and M. Ernzerhof, Erratum: Hybrid functionals based on a screened Coulomb potential, *J. Chem. Phys.* 124(21), 219906 (2006) (*J. Chem. Phys.* 118, 8207 (2003))
39. A. Kahn, Fermi level, work function and vacuum level, *Mater. Horiz.* 3(1), 7 (2016)
40. J. P. Perdew, K. Burke, and M. Ernzerhof, Generalized gradient approximation made simple, *Phys. Rev. Lett.* 77(18), 3865 (1996)
41. S. Grimme, Semiempirical GGA-type density functional constructed with a long-range dispersion correction, *J. Comput. Chem.* 27(15), 1787 (2006)
42. M. Dion, H. Rydberg, E. Schroder, D. C. Langreth, and B. I. Lundqvist, van der Waals density functional for general geometries, *Phys. Rev. Lett.* 92(24), 246401 (2004)
43. M. Jourshabani, B. K. Lee, and Z. Shariatinia, From traditional strategies to Z-scheme configuration in graphitic carbon nitride photocatalysts: Recent progress and future challenges, *Appl. Catal. B* 276, 119157 (2020)
44. P. Zhou, J. Yu, and M. Jaroniec, All-solid-state Z-scheme photocatalytic systems, *Adv. Mater.* 26(29), 4920 (2014)

45. Y. Tachibana, L. Vayssieres, and J. R. Durrant, Artificial photosynthesis for solar water-splitting, *Nat. Photonics* 6(8), 511 (2012)
46. S. J. A. Moniz, S. A. Shevlin, D. J. Martin, Z. X. Guo, and J. Tang, Visible-light driven heterojunction photocatalysts for water splitting — a critical review, *Energy Environ. Sci.* 8(3), 731 (2015)
47. J. K. Hyun, S. Zhang, and L. J. Lauhon, Nanowire heterostructures, *Annu. Rev. Mater. Res.* 43(1), 451 (2013)
48. J. Fu, Q. Xu, J. Low, C. Jiang, and J. Yu, Ultrathin 2D/2D WO_3/g-C_3N_4 step-scheme H_2-production photocatalyst, *Appl. Catal. B* 243, 556 (2019)
49. T. Su, Q. Shao, Z. Qin, Z. Guo, and Z. Wu, Role of interfaces in two-dimensional photocatalyst for water splitting, *ACS Catal.* 8(3), 2253 (2018)
50. Q. L. Xu, L. Y. Zhang, J. G. Yu, S. Wageh, A. A. Al-Ghamdi, and M. Jaroniec, Direct Z-scheme photocatalysts: Principles, synthesis, and applications, *Mater. Today* 21(10), 1042 (2018)
51. X. Li, J. Yu, J. Low, Y. Fang, J. Xiao, and X. Chen, Engineering heterogeneous semiconductors for solar water splitting, *J. Mater. Chem. A* 3(6), 2485 (2015)
52. X. Chen, S. Shen, L. Guo, and S. S. Mao, Semiconductor-based photocatalytic hydrogen generation, *Chem. Rev.* 110(11), 6503 (2010)
53. Z. Sun, N. Talreja, H. Tao, J. Texter, M. Muhler, J. Strunk, and J. Chen, Catalysis of carbon dioxide photoreduction on nanosheets: Fundamentals and challenges, *Angew. Chem. Int. Ed.* 57(26), 7610 (2018)
54. K. Ren, W. Tang, M. Sun, Y. Cai, Y. Cheng, and G. Zhang, A direct Z-scheme PtS_2/arsenene van der Waals heterostructure with high photocatalytic water splitting efficiency, *Nanoscale* 12(33), 17281 (2020)
55. I. Man, H. Su, F. Calle-Vallejo, H. Hansen, J. Martinez, N. Inoglu, J. Kitchin, T. Jaramillo, J. Norskov, and J. Rossmeisl, Universality in oxygen evolution electrocatalysis on oxide surfaces, *ChemCatChem* 3(7), 1159 (2011)
56. R. Zhang, L. Zhang, Q. Zheng, P. Gao, J. Zhao, and J. Yang, Direct Z-scheme water splitting photocatalyst based on two-dimensional van der Waals heterostructures, *J. Phys. Chem. Lett.* 9(18), 5419 (2018)
57. X. Niu, X. Bai, Z. Zhou, and J. Wang, Rational design and characterization of direct Z-scheme photocatalyst for overall water splitting from excited state dynamics simulations, *ACS Catal.* 10(3), 1976 (2020)
58. C. Jin, E. Y. Ma, O. Karni, E. C. Regan, F. Wang, and T. F. Heinz, Ultrafast dynamics in van der Waals heterostructures, *Nat. Nanotechnol.* 13(11), 994 (2018)
59. R. Long and O. V. Prezhdo, Quantum coherence facilitates efficient charge separation at a MoS_2/$MoSe_2$ van der Waals junction, *Nano Lett.* 16(3), 1996 (2016)